

A Low-Cost Dual Layer Deca-Dodecasil 3 Rhombohedral-Alumina Hollow Fiber for CO₂/CH₄ Separation

Renan Fraga Barbosa^{a*} , Alberto Claudio Habert^a, Cristiano Piacsek Borges^a

^aUniversidade Federal do Rio de Janeiro (UFRJ), Instituto Alberto Luiz Coimbra de Pós-Graduação e Pesquisa de Engenharia (COPPE), Programa de Engenharia Química, Rio de Janeiro, RJ, Brasil.

Received: September 29, 2023; Revised: December 13, 2023; Accepted: December 21, 2023

Membrane technology offers solutions for separation of complex gas mixtures. Therefore, new efficient and durable membranes are required to produce gas permeation modules with high area/volume for CO₂ removal from natural gas. This study aims to develop cost-effective zeolite DD3R alumina composite hollow fibers to achieve these process requirements. A porous hollow fiber support from low-cost alumina was prepared via phase inversion followed by thermal treatment. DD3R zeolite seeds were then implanted over the surface of the microporous hollow fibers to form a selective layer by hydrothermal synthesis. The thickness of the selective layer was controlled by the seed concentration, which also affected the crystal intergrowth and competing zeolite phase formation, Sigma-2, which influenced the membrane performance. A reduced-diameter composite DD3R-alumina hollow fiber was obtained with a selectivity of 203 and a CO₂ permeance of 5.4 x 10⁻⁸ mol m⁻² s⁻¹ Pa⁻¹ at a pressure of 2 bar.

Keywords: DD3R zeolite membrane, Alumina Hollow fiber, CO₂-CH₄ separation, Molecular sieving

1. Introduction

Membranes have been used for CO₂ removal of natural gas purification since the mid-80's when cellulose acetate asymmetric membranes boosted this particular market. Since then, polymeric membranes have been well established for industrial gas-separation processes. However, these membranes have operational limitations, including reduced selectivity due to CO₂-induced plasticization, decreased permeance due to membrane compaction and aging, and low resistance to rupture at high pressures. As an alternative to polymeric membranes, zeolite membranes are excellent candidates for CO₂/CH₄ separation due to their high selectivity and permeance. The outstanding performance of zeolite membranes is attributed to the strong affinity of zeolites for CO₂, leading to the preferential adsorption of CO₂ over CH₄, combined with the molecular sieving separation provided by the zeolite microporous structure¹⁻⁴.

Among the zeolites used for membrane production, decadodecasil 3 rhombohedral (DD3R) zeolite stands out because of its unique pore opening (0.36×0.44 nm), resulting in an effective pore diameter of 0.36 nm, which is in the range of the kinetic diameters of CO₂ (0.33 nm) and CH₄ (0.38 nm). The first DD3R zeolite membrane has been developed by Tomita et al.⁵ on an alumina tubular support to separate the CO₂/CH₄ mixture, achieving a selectivity of 220 and CO₂ permeance of 7 x 10⁻⁸ mol m⁻² s⁻¹ Pa⁻¹. Continuing Tomita et al.⁵ works, Himeno et al.³ produced a DD3R selective layer on an alumina asymmetric tubular membrane support, achieving a similar CO₂/CH₄ selectivity of 200, with a permeance six times higher. Recently, Wang et al.⁴ developed a new detemplation method for DD3R zeolite through low-temperature calcination in an ozone atmosphere,

drastically reducing the number of defects in the selective layer. Using this technique, the authors prepared a DD3R membrane on an asymmetric alumina four-channel hollow fiber support.

However, despite the advancements in DD3R membrane preparation owing to the ozone detemplating method, large-scale production remains a challenge because of the issues associated with the fabrication process. These include the formation of competitive phases, like Dodecasil-1H (DOH) and Sigma-2 (SGT) zeolites^{6,7}, and the development of intercrystalline defects, which reduce the selectivity at higher pressures, as observed by Wang et al.⁸, where the selectivity decreased from 200 at 1.4 bar to 15 at 40 bar.

Another challenge lies in the production cost of zeolite membrane modules, which is mostly related to membranes, sealing materials, and low packing density. Notably, up to 70% of the production cost is attributed to the choice of membrane support, which can be reduced by selecting cheaper raw materials⁹. Another approach to reduce the module cost is to increase the membrane density packing, that is, aiming at a module with a higher membrane surface area per unit volume. This can be achieved by using a hollow fiber support instead of tubular membranes, resulting in an increase in the density packing from 30 to 250 m²·m⁻³ for tubular supports and up to 1000 m²·m⁻³ for hollow fibers¹⁰⁻¹³.

The purpose of this study was to prepare and characterize a low-cost DD3R zeolite composite membrane selective for CO₂ in a hollow fiber configuration. There are not many reports in the literature on such a single selective hollow fiber. The 2 steps fabrication technique involves the preparation of an affordable alumina microporous support to be coated with a locally synthesized DD3R zeolite layer.

*e-mail: renan@peq.coppe.ufrj.br

Evaluation of the permeability of these membranes will provide criteria for the effectiveness of the technique and its potential use in permeation modules for gas separation processes.

2. Experimental

2.1. Chemicals

Commercial alumina powder (Solotest, Brazil), with an average particle size of 4 μm was used to prepare the hollow fibers. N-methyl-2-pyrrolidinone (NMP, Isofar), polyethersulfone (PES, Solvay), and polyvinylpyrrolidone (PVP, K90, Sigma-Aldrich) were the components of the dope mixture prepared for fiber extrusion as solvent, polymeric binder, and dispersant additive, respectively.

To produce DD3R seeds and the zeolite selective layer, colloidal silica, Ludox HS-40 (Sigma-Aldrich) was used as the silica source, while 1-adamantanamine (ADA, 99%, Shanghai Tianqi Chemical Limited) was used as the structure-directing agent. Ethylenediamine (EN, Sigma-Aldrich) and potassium fluoride (KF, Quimibras) were used as mineralizing agents.

2.2. Preparation of alumina hollow fibers supports

Low-cost alumina hollow fiber supports were produced using phase inversion and sintering techniques. To achieve this, a dope mixture was prepared by dissolving the polymers in a solvent with high-speed mechanical stirring for 3 h. Subsequently, alumina powder was gradually added into the solution under mechanical stirring for 48 h to ensure dispersion of the alumina powder. This suspension was then transferred to a stainless-steel reservoir and degassed for 12 h. After degassing, the spinning suspension was pressurized with nitrogen and extruded through a tube-in-orifice spinneret with an outer diameter of 3.8 mm and inner diameter of

1.6 mm. Water was used as both the coagulant fluid and the coagulation bath. The composition of the spinning suspension and the extrusion conditions are detailed in Table 1, and Figure 1 shows the experimental apparatus for hollow fiber preparation.

The precursor hollow fibers were kept in water for 24 h to remove residual solvent. The samples were cut and dried at room temperature. The fibers were then sintered in a tubular electric furnace. A three-stage temperature procedure was employed to preserve the membrane structure and prevent defects. Initially, the temperature gradually increased from 25 $^{\circ}\text{C}$ to 200 $^{\circ}\text{C}$ at a rate of 2 $^{\circ}\text{C}/\text{min}$, and this level was maintained for 1 h to eliminate the residual solvent. The temperature was then increased to 600 $^{\circ}\text{C}$ at a rate of 2 $^{\circ}\text{C}/\text{min}$ and maintained for 2 h to incinerate the polymers. Subsequently, the temperature was further elevated to 1,550 $^{\circ}\text{C}$ at a rate of 5 $^{\circ}\text{C}/\text{min}$ and was sustained for 4 h to sinter the alumina particles. Finally, the furnace was cooled slowly to 25 $^{\circ}\text{C}$.

Table 1. Spinning conditions of alumina hollow fibers.

Suspension composition (wt.%)	
Al_2O_3	52.0
PES	6.0
PVP	0.5
NMP	41.5
Spinning suspension flow rate (ml/min)	4.0
Internal coagulant flow rate (ml/min)	3.0
Air gap (cm)	3.5

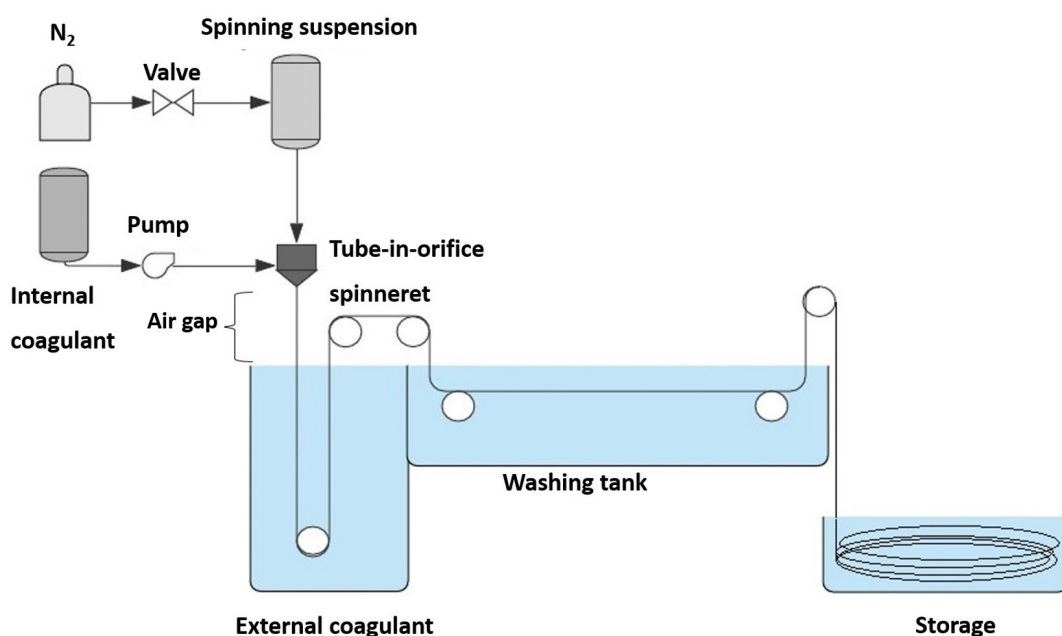


Figure 1. Spinning process to prepare a precursor alumina hollow fiber.

2.3. Synthesis of DD3R zeolite crystals

DD3R crystals were prepared using the methodology outlined by Peng et al.¹⁴, which consists of generating a pristine amorphous solid that accelerates the synthesis of the DD3R zeolite. This amorphous solid was prepared by mixing the reactants 1SiO₂:4.04 EN:0.47 ADA:112 H₂O (molar ratio) in deionized water for 3 h. Subsequently, the formed gel was introduced into a stainless-steel autoclave for 48 h at 160 °C. The resulting product was washed and dried for use as a precursor for the DD3R zeolite. To obtain zeolite crystals, another hydrothermal synthesis step was carried out using a reaction medium with a composition of 1.0SiO₂:0.5 ADA:1 KF:80 H₂O (molar ratio) and 0.1 wt. % of the synthesized precursor, maintaining the same reaction conditions as in the previous synthesis. After the reaction time had elapsed, the crystals were washed, dried, and calcined at 700 °C for 6 h to remove ADA from the zeolite pores. Finally, the crystals were ball milled to reduce their particle size.

2.4. Preparation of the DD3R zeolite membrane

The DD3R zeolite membranes were synthesized using a secondary growth method. Initially, the ends of the prepared alumina hollow fibers were sealed using Teflon tape. These fibers were then immersed in a suspension of DD3R crystals a source of seeds for 30 s to ensure the insertion of the crystals into the support membranes. The seeded supports were dried at 100 °C for 1 h.

To produce the DD3R zeolite layer, a synthesis gel was formulated with a composition based on the work of Hayakawa and Himeno¹⁵, that is, 1SiO₂: 0.056 ADA:0.056 KF:52 H₂O (molar ratio). The gel was prepared by mixing reactants in distilled water for 3 h. It was then placed in a stainless-steel autoclave containing the previously seeded hollow fibers. The reaction mixture was then maintained at 140 °C for 24 h.

The recently prepared DD3R-alumina hollow fibers were washed and dried at 100 °C for 1 h. The membranes were calcined in a tubular oven under an ozone environment for the detemplation of zeolite pores, following the methodology described by Wang et al.⁴. The calcination process was carried out at 200 °C, maintaining a continuous oxygen flow rate of 1 L/min, containing 56 mg/L ozone, for a certain period.

2.5. Characterization

The morphologies of the DD3R crystals, the surface and cross-sectional areas of the alumina hollow fiber support, and the DD3R-alumina hollow fibers were observed using Scanning Electron Microscopy (SEM, TESCAN VEGA 3). The crystal phase was identified by X-ray diffraction (XRD, Panalytical, AERIS) with Cu K α radiation (1.54050 Å) in the 2 θ range of 5–90°. To evaluate the endurance of the alumina hollow fiber support, bending strength tests were conducted using a tensile tester (Stable Micro Systems, TA HD plus) equipped with a 0.5 kN load cell. The mechanical strength σ_F (Pa) was calculated using Equation 1:

$$\sigma_F = \frac{8.F.L.D_e}{\pi(D_o^4 - D_i^4)} \quad (1)$$

where F (N) denotes the load measured at the fracture point. L is the distance (m) between the supports and Do (m) and Di (m) represent the outer and inner diameters of the hollow fiber, respectively.

Adsorption tests were conducted to evaluate the DD3R affinity for CO₂ and CH₄ using an apparatus consisting essentially of a gas-pressurized cell connected to a pressure transducer to measure the pressure decay. The amount of gas adsorbed on the zeolite was determined using Equation 2:

$$S = \frac{\Delta P.V.M}{R.T.m} \quad (2)$$

where S is the gas adsorbed in the zeolite, ΔP (bar) is the gas pressure drop in the pressurized cell, V (cm³) is the cell volume, M(g/mol) is the molar mass of the gas, and R is the universal gas constant (cm³.bar.mol⁻¹.K⁻¹), T (K) is the cell temperature, and m (Kg) is the sample mass inside the cell.

2.6. Pure gas permeation

Dead-end stainless-steel modules were used for the alumina support and DD3R-alumina hollow fibers. The permeance (p/l) of the alumina support was determined using a gas flow meter gauge, whereas for the DD3R-alumina membrane, the permeance was measured using a pressure transducer by applying Equation 3.

$$\frac{p}{l} = \frac{dP}{dt} \cdot \frac{V_s}{A.\Delta P} \cdot \frac{T_{CNTP}}{T.P_{CNTP}} \quad (3)$$

where dP/dt represents the permeate pressure variation over time, V_s is the permeate chamber volume, A is the effective membrane area, T is the operating temperature, and T_{CNTP} and P_{CNTP} are the temperature and pressure under normal conditions, respectively.

The binary ideal selectivity ($\alpha_{i,j}$), measured through the ratio of the permeance of pure gases i and j, was calculated using Equation 4:

$$\alpha_{i,j} = \frac{\left(\frac{p}{l}\right)_i}{\left(\frac{p}{l}\right)_j} \quad (4)$$

3. Results and Discussion

3.1. Preparation and characterization of alumina hollow fibers

After preparing the precursor fibers and subsequent sintering, the morphology of the alumina hollow fibers, as revealed by scanning electron microscopy, showed that this precursor membrane had a porous morphology (Figure 2), which remained unchanged after sintering, as desired. Additionally, there was a 30% reduction in the diameter of the fibers compared to that of the precursor fibers after sintering. All hollow fibers produced by the phase inversion technique displayed walls with a uniform symmetric sponge-like morphology, as shown in Figure 3b. This is attributed to the fast precipitation rate of the polymer/alumina suspension, which is strongly influenced by viscosity.

Abdulhameed et al.¹⁶ observed a similar membrane morphology using kaolin particles with a range of 2–4 μm so, it is also reasonable to admit that the low-cost larger size alumina selected in the present investigation is at the origin of this morphology. The average size of the alumina particles in Figure 3a is approximately 4 μm and shows a reasonably wide size distribution. In general, the addition of insoluble particles to a polymer solution leads to higher viscosity. However, large particles have a minor effect on suspension viscosity. Several authors^{17–19} have correlated membrane morphology with the precipitation rate in phase-inversion membrane fabrication. Faster precipitation favors a sponge-like pore structure because of the fast mass transfer occurring during solvent/non-solvent exchange.

These inorganic membranes exhibited a remarkable flexural strength of 177.5 ± 27 MPa, as confirmed through

a three-point bending test. Gitis and Rothenberg²⁰ suggest that a particle size of 2 μm represents the upper limit for ensuring a robust membrane. However, owing to the broad particle size distribution, it is likely that smaller particles are accommodated among the larger particles, resulting in enhanced material packing according to the sphere packing theory²¹. It is worth emphasizing that the mechanical strength of the membranes can be attributed to their sponge-like morphology and to the high sintering temperature, both of which promote material densification and contribute to a pore diameter reduction. Analysis of the SEM images also showed that the alumina hollow fibers, meant for the support, had a mean pore diameter of 0.7 μm . The pore distribution analysis confirmed that the hollow alumina fibers had pores consistent with a microfiltration membrane, with a measured a high nitrogen permeance of 4.6×10^{-5} ($\text{mol m}^{-2} \text{s}^{-1} \text{Pa}^{-1}$).

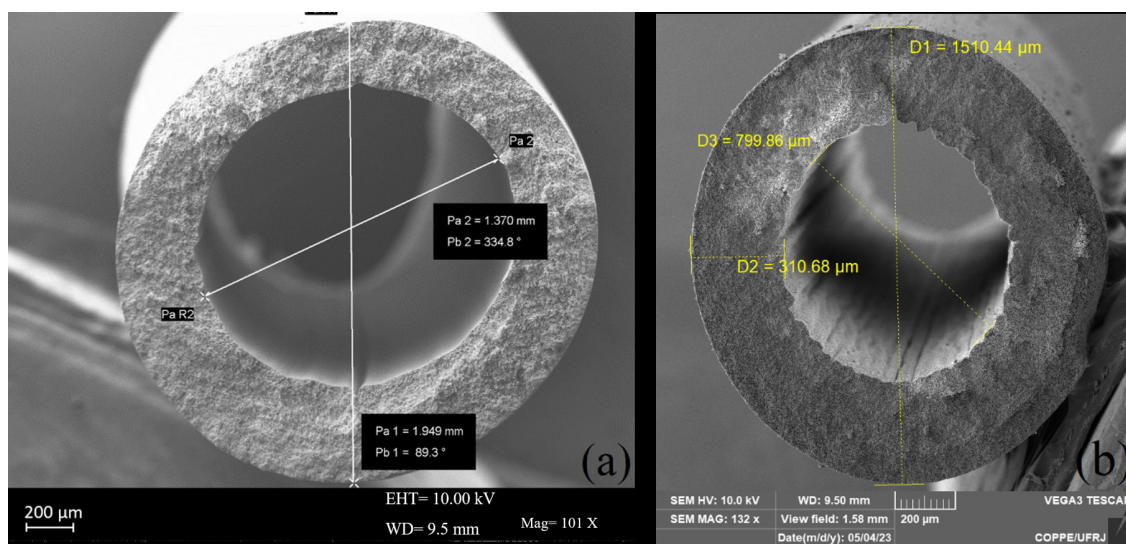


Figure 2. SEM image of the cross-section of: (a) precursor hollow fiber, (b) alumina hollow fiber.

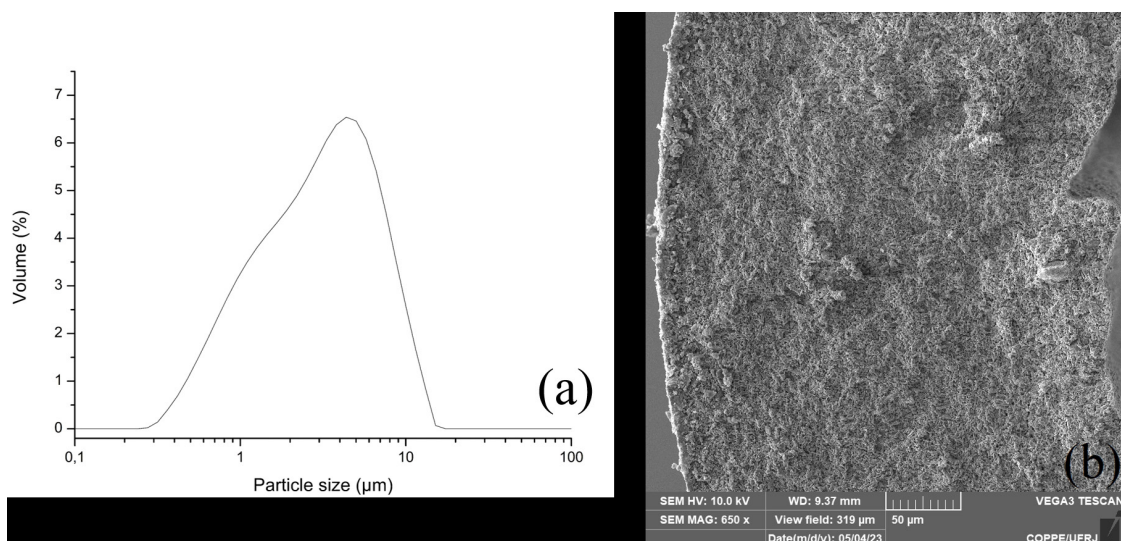


Figure 3. (a) Alumina particle size distribution. (b) SEM of the alumina hollow fiber cross-section.

3.2. Synthesis of DD3R zeolite crystals and fabrication of DD3R-alumina hollow fibers

The DD3R zeolite crystals were successfully produced in just 4 days using the methodology of Peng et al.¹⁴, obtaining large octahedral crystals (Figure 4a). The crystals were analyzed by X-ray diffractometry, and the diffractograms are shown in Figure 4b. A strong correlation was observed between the experimental data for the synthesized zeolite and the DD3R standard pattern. The absence of significant peaks in the line representing the difference between the experimental and standard data indicates the successful production of a predominantly pure DD3R zeolite phase. The gas sorption experiment was conducted with DD3R crystals, resulting in a calculated adsorption coefficient of 28.2 g of

CO₂ per kg of DD3R zeolite, which is 6 times higher than the adsorption coefficient of CH₄, indicating that the zeolite has a strong preference for CO₂ over CH₄ (see Appendix A).

DD3R crystals were ball-milled for use as seeds, reducing their size to an average diameter of 4.9 μm. Two suspensions were prepared, with seed concentration of 0.5 wt. % and 0.25 wt.%, respectively. The seeds were then implanted in the alumina hollow fiber and transferred to a stainless-steel autoclave containing the synthesis gel to form a DD3R selective layer by hydrothermal synthesis. Successive adjustments in the seeding technique enabled the reduction of the seed layer on the substrate, thereby reducing the final thickness of the selective layer, as shown in the SEM images of the cross-sections of the C1-DD3R, C2-DD3R, and C3-DD3R membranes (Figure 5).

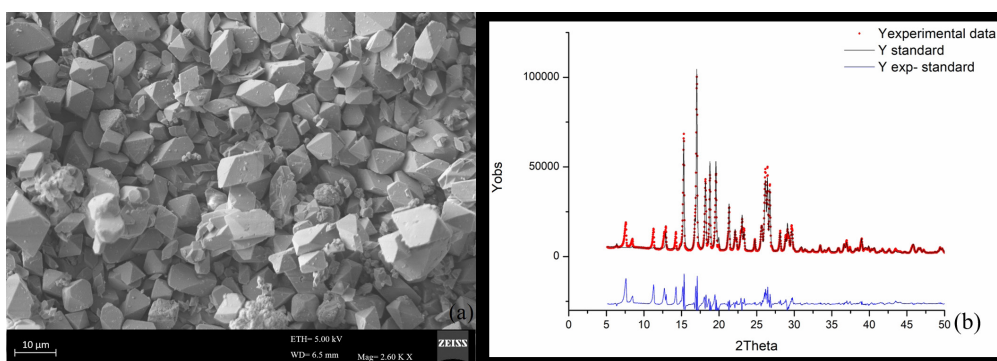


Figure 4. (a) SEM image of DD3R zeolite crystals. (b) Diffractogram of DD3R zeolite crystals and comparison with standard DD3R pattern.

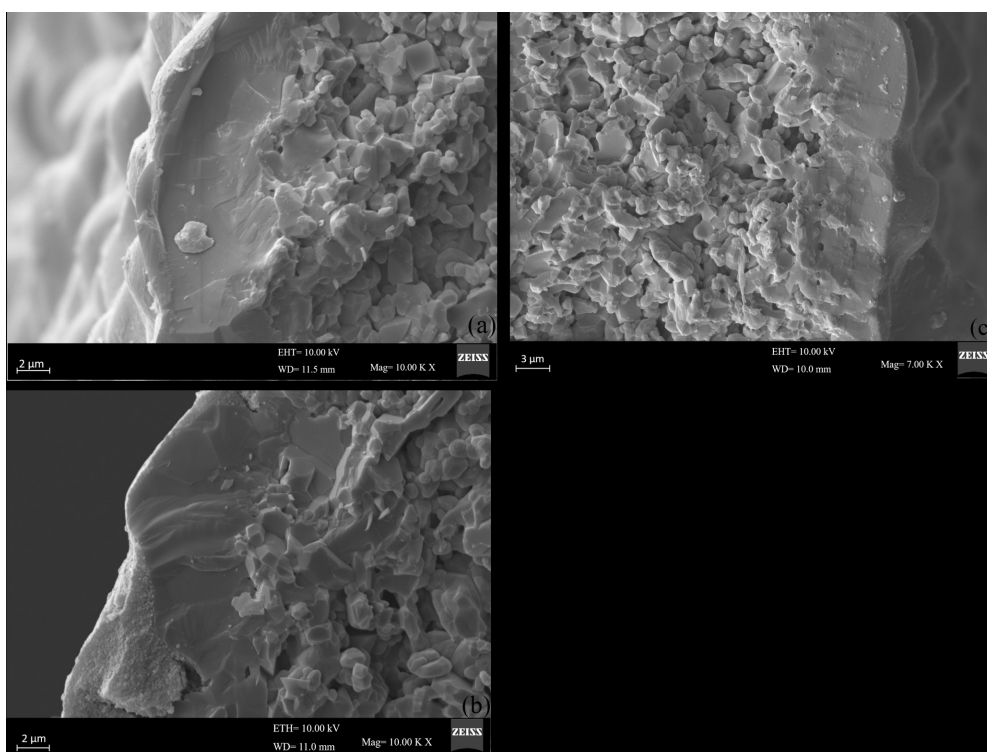


Figure 5. SEM image of the cross-section of membranes (a) C1-DD3R, (b) C2-DD3R and (c) C3-DD3R.

The resulting membranes exhibited non-uniform layers, provoked by the wide particle-size distribution of the seed, creating challenges for the accurate measurement of the thickness of each membrane. The average thickness of the membranes was measured and are presented in Table 2. Notably, a smaller quantity of seeds implanted in the membrane support led to reduced crystal intergrowth in the DD3R selective layer, and consequently, to the formation of a thinner selective layer. Wang et al.⁸ also confirmed the proportionality between the seed concentration and zeolite layer thickness.

In addition to controlling the selective layer thickness, controlling the formation of distinct zeolite phases is crucial. However, despite conducting the hydrothermal reaction at a lower temperature, the formation of a competing crystalline phase, the zeolite SGT, was observed on the membrane surface,

as illustrated in Figure 6. The SGT phase is characterized by sphere-like structures with a pore size of approximately 0.3 nm, while DD3R has octahedron-like structures and a pore size of 0.36 nm⁸. Analysis of the surfaces of the C1-DD3R and C2-DD3R membranes revealed that the SGT zeolite appear as clusters, covering a large area of the selective layer. However, as it can be observed in Figure 6d, the C2-DD3R had smaller clusters, indicating less formation of the SGT zeolite. This may be attributed to the reduction of the seed concentration from 0.5%wt to 0.25%. A decrease in the dip-coating time also reduced the intergrowth of the DD3R phase, as shown in Figure 6c for the C3-DD3R membrane. Therefore, it may be concluded that a decrease in the seed amount implanted on the membrane support leads to a relatively limited intergrowth of the DD3R zeolite layer, which may result in the appearance of defects.

Table 2. Synthesis condition and average thickness for DD3R selective layers.

Batch	Seed concentration (%)	Dip coating time (s)	DD3R layer thickness (μm)
C1-DD3R	0.50	30	9.2
C2-DD3R	0.25	30	8.1
C3-DD3R	0.25	15	6.4

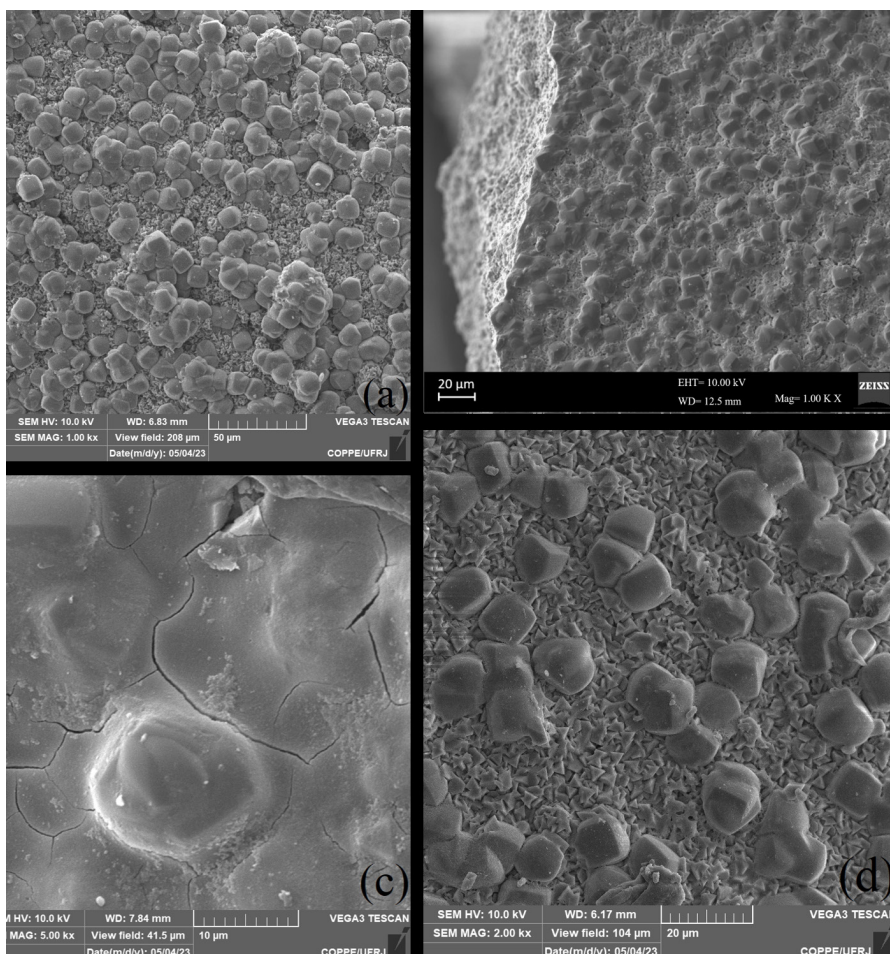


Figure 6. SEM image of membranes surface (a) C1-DD3R, (b) C2-DD3R, (c) C3-DD3R, and (d) High magnification of C2-DD3R.

During the detemplation stage, it was noticed that 8 days were necessary to remove ADA from the pores of the C1-DD3R membranes, while for C2-DD3R, it took 5 days for the activation process. These longer oxidation times were required because of the thickness of the membranes, as described by Xu et al.²², who demonstrated that the degradation time is proportional to the membrane thickness. Therefore, owing to its lower membrane thickness, C2-DD3R had a faster activation stage than C1-DD3R. In addition, C2-DD3R also has a lower formation of SGT zeolite on its surface, resulting in a higher free surface area and, consequently, better contact with the ozone stream.

3.3. Gas permeation

Table 3 presents the performance of the membranes produced from the C1-DD3R and C2-DD3R batches. A significant variation was observed between the membrane permeances of both batches. This variation is likely attributable to differences in the DD3R zeolite layer thickness and the amount of SGT zeolite on the selective layer, confirming the challenges in replicating the membrane preparation process, as reported in the literature. C1-DD3R presented higher selectivity than C2-DD3R, which was attributed to the larger intergrowth of DD3R crystals, resulting in membranes with fewer defects. However, this condition favors membranes with a lower permeance. On the other hand, reducing the number of seeds implanted in the support, as in C2-DD3R synthesis, diminishes the crystal intergrowth and may lead to defect formation and a significant decrease in selectivity.

As shown in Table 3, the C2-DD3R membranes exhibited significant fluctuations in selectivity, which may have resulted from intercrystalline defects.

It should also be mentioned that a higher amount of SGT zeolite over the selective layer also provokes a reduction in permeance, which can also explain the lower permeance of batch C1-DD3R compared to batch C2-DD3R. The SGT zeolite has a pore diameter of 0.30 nm, which is smaller than the kinetic diameters of CO₂ (0.33 nm) and CH₄ (0.38 nm). Therefore, this zeolite is mostly impermeable to these gases

Membranes C2-DD3R-1 and C2-DD3R-3 were selected for gas permeation under different pressure conditions to evaluate the quality of the produced selective layers. It is known that DD3R zeolite has a high affinity for CO₂, as confirmed by adsorption tests, which contributes to the high selectivity of CO₂ over CH₄, particularly at low pressures. Preferential CO₂ adsorption favors its transport, even through minor intercrystalline defects, thereby increasing the membrane selectivity. However, an increase in feed pressure significantly reduces membrane selectivity because of the higher contribution of non-selective permeation through defects and also to the reduction of CO₂ permeance due to the saturation of the DD3R zeolite active sites. This phenomenon is evident in the gas permeation test with C2-DD3R-1, as shown in Figure 7a, where the presence of a more significant number of defects in this membrane leads to a drastic drop in selectivity, decreasing from 44 to 27 as the pressure increases from 1 to 2 bar.

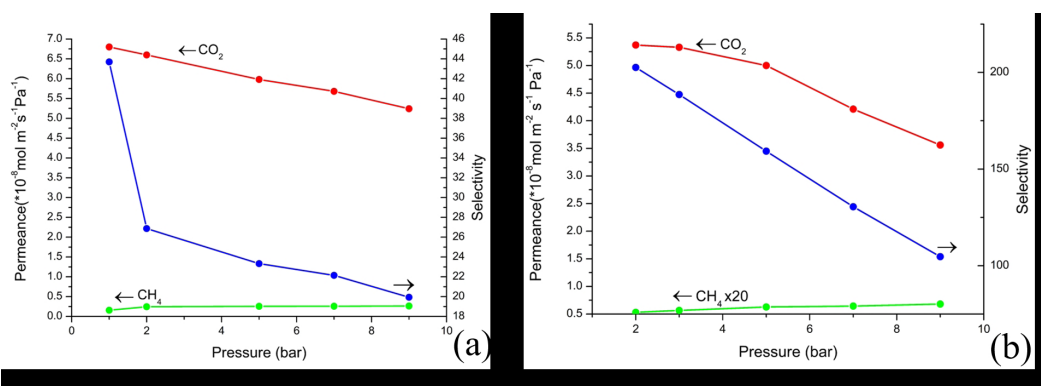


Figure 7. Effect of feed pressure on CO₂ and CH₄ permeation in DD3R/Alumina hollow fiber membranes (a) C2-DD3R-1, and (b) C2-DD3R-3.

Table 3. Separation performance* of DD3R-alumina hollow fiber.

Membrane	Permeance CO ₂ × 10 ¹⁰ (mol m ⁻² s ⁻¹ Pa ⁻¹)	Selectivity CO ₂ /CH ₄
C1-DD3R-1	134	277
C1-DD3R-2	74	150
C1-DD3R-3	7	208
C2-DD3R-1	660	27
C2-DD3R-2	807	33
C2-DD3R-3	536	203
C2-DD3R-4	114	294
C2-DD3R-5	315	84

*Permeation conditions: 23°C; pressure difference: 1 bar (C1-DD3R permeation) and 2 bar (C2-DD3R permeation).

Table 4. Performance comparison of DD3R zeolite composite membranes.

Membrane support	Pore diameter (μm)	Pressure (bar)	CO_2 Permeance $\times 10^8$ ($\text{mol m}^{-2} \text{s}^{-1} \text{Pa}^{-1}$)	Selectivity (CO_2/CH_4)	Ref.
Tubular ²	0.6	5	7	220 (50/50)	⁵
Tubular ¹	0.2	2	42	340 (ideal)	³
Four-channel HF ²	0.5	5	3	190(50/50)	⁴
Tubular ¹	0.2	1,4	47	190 (50/50)	⁸
Flat Sheet ¹	-	1	31	536 (50/50)	²³
Tubular ¹	0,2	3	6.2	400 (50/50)	¹⁵
HF ²	0.7	2	5	203 (ideal)	This work
HF ²	0.7	9	4	105 (ideal)	This work

¹Asymmetric membrane. ²Symmetric membrane. HF – Hollow fiber.

Analysis of the gas permeation exhibited in Figure 7b for C2-DD3R-3 also shows a reduction in CO_2 permeance with pressure, due to the saturation of the DD3R zeolite. Nevertheless, the CH_4 permeance remained very low when the operating pressure was increased, confirming that the selective layer was probably quite defect-free. Even at a higher pressure of 9 bar, the membrane maintained high performance, achieving a selectivity of 105 and a permeance of 106 GPU.

3.4. Comparison with other DD3R membranes

To better evaluate the performance of the DD3R-Alumina membranes prepared in this study, Table 4 lists the results for similar membranes selected from reliable data reported in the literature. One should be aware of any operating pressure effect, as well as of the membrane configuration and nature of the precursor support, as they may compromise direct comparisons. However, the collected data are an indication of the progress achieved in this work, as the C2-DD3R-3 Alumina hollow fiber membrane showed notable selectivity, even at higher feed pressures. Composite membranes prepared using asymmetric (multilayered) supports exhibited a higher permeance than those fabricated with symmetric supports. It is also worth observing that most of the membranes shown in Table 4 were prepared using commercial porous support. In contrast, in this study, high-quality DD3R-alumina hollow fiber membranes were obtained by a simple and scalable method, allowing therefore the manufacture of permeation modules with high packing density, that is to say, substantial surface areas, compensating therefore, by large, their relatively lower permeance in comparison with other candidates of Table 4.

4. Conclusions

It is possible to prepare CO_2 selective composite low-cost DD3R-alumina hollow fiber membranes in two steps: microporous support fabrication, followed by the deposition of a zeolite layer over the external surface of the fiber. This structure was confirmed using SEM. Commercial alumina micrometric powder (in the range of $4 \mu\text{m}$) proved to be an excellent raw material for manufacturing microporous hollow fiber supports by a phase inversion wet extrusion technique. The extrusion of a polymer/alumina suspension, followed by thermal sintering, led to the formation of hollow fibers with a homogeneous and uniform sponge-like morphology.

These supports exhibited a high permeance of 4.6×10^{-5} ($\text{mol m}^{-2} \text{s}^{-1} \text{Pa}^{-1}$) with a noteworthy flexural strength of 177.5 ± 27 MPa. The thickness of the DD3R selective layer was adjusted by the number of seeds implanted in the support, which was controlled by the seed concentration of the implant suspension. In addition to the membrane thickness, the number of seeds implanted over the support also contributes to the formation of an additional phase, (SGT zeolite) on the membrane surface, a phenomenon to avoid as it will affect the effectiveness of the membrane. A high-performance membrane was obtained with a selectivity of 203 and CO_2 permeance of $5.4 \times 10^{-8} \text{ mol m}^{-2} \text{ s}^{-1} \text{ Pa}^{-1}$ at a pressure of 2 bar. These results clearly indicate the potential of DD3R-alumina hollow fibers as candidates for the manufacture of permeation modules with a high packing density for CO_2/CH_4 separation.

5. Acknowledgements

The authors gratefully acknowledge financial support from the Coordenação de Aperfeiçoamento de Pessoal de Nível Superior – Brasil (CAPES).

6. References

- Martin-Gil V, Ahmad MZ, Castro-Muñoz R, Fila V. Economic framework of membrane technologies for natural gas applications. *Separ Purif Rev.* 2019;48(4):298-324. <http://dx.doi.org/10.1080/015422119.2018.1532911>.
- Hsieh HP. *Inorganic membranes for separation and reaction.* Amsterdam: Elsevier; 1996.
- Himeno S, Tomita T, Suzuki K, Nakayama K, Yajima K, Yoshida S. Synthesis and permeation properties of a DDR-type zeolite membrane for separation of CO_2/CH_4 gaseous mixtures. *Ind Eng Chem Res.* 2007;46(21):6989-97.
- Wang L, Zhang C, Gao X, Peng L, Jiang J, Gu X. Preparation of defect-free DDR zeolite membranes by eliminating template with ozone at low temperature. *J Membr Sci.* 2017;539:152-60. <http://dx.doi.org/10.1016/j.memsci.2017.06.004>.
- Tomita T, Nakayama K, Sakai H. Gas separation characteristics of DDR type zeolite membrane. *Microporous Mesoporous Mater.* 2004;68(1-3):71-5.
- Güçüyener C, Van Den Bergh J, Joaristi AM, Magusin PCMM, Hensen EJM, Gascon J, et al. Facile synthesis of the DD3R zeolite: performance in the adsorptive separation of buta-1,3-diene and but-2-ene isomers. *J Mater Chem.* 2011;21(45):18386-97.
- Vo PNX, Phan PD, Ngo PT, Le-Phuc N, Tran TV, Luong TN, et al. Memory effect in DDR zeolite powder and membrane synthesis. *Microporous Mesoporous Mater.* 2019;279:142-52. <http://dx.doi.org/10.1016/j.micromeso.2018.12.031>.

8. Wang M, Bai L, Li M, Gao L, Wang M, Rao P, et al. Ultrafast synthesis of thin all-silica DDR zeolite membranes by microwave heating. *J Membr Sci.* 2019;572:567-79. <http://dx.doi.org/10.1016/j.memsci.2018.11.049>.
9. Rani SLS, Kumar RV. Insights on applications of low-cost ceramic membranes in wastewater treatment: a mini-review. *Case Stud Chem Environ Eng.* 2021;4:100149.
10. Wang X, Jiang J, Liu D, Xue Y, Zhang C, Gu X. Evaluation of hollow fiber T-type zeolite membrane modules for ethanol dehydration. *Chin J Chem Eng.* 2017;25(5):581-6.
11. Caro J, Noack M. Zeolite membranes - status and prospective. In: Ernst S, editor. *Advances in nanoporous materials.* Vol. 1. Amsterdam: Elsevier; 2010. p. 1-96.
12. Xu X, Yang W, Liu J, Lin L, Stroh N, Brunner H. Synthesis of NaA zeolite membrane on a ceramic hollow fiber. *J Membr Sci.* 2004;229(1-2):81-5.
13. Shu X, Wang X, Kong Q, Gu X, Xu N. High-flux MFI zeolite membrane supported on ysz hollow fiber for separation of ethanol/water. *Ind Eng Chem Res.* 2012;51(37):12073-80.
14. Peng A, Lu X, Ma R, Fu Y, Wang S, Zhu W. Comparative study on different strategies for synthesizing all-silica DD3R zeolite crystals with a uniform morphology and size. *RSC Adv.* 2020;10(46):27523-30.
15. Hayakawa E, Himeno S. Synthesis of a DDR-type zeolite membrane by using dilute solutions of various alkali metal salts. *Separ Purif Tech.* 2019;218:89-96.
16. Abdulhameed MA, Othman MHD, Ismail AF, Matsuura T, Harun Z, Rahman MA, et al. Preparation and characterisation of inexpensive porous kaolin hollow fibre as ceramic membrane supports for gas separation application. *J Aust Ceram Soc.* 2017;53(2):645-55.
17. Abdullah N, Rahman MA, Othman MHD, Ismail AF, Jaafar J, Aziz AA. Preparation and characterization of self-cleaning alumina hollow fiber membrane using the phase inversion and sintering technique. *Ceram Int.* 2016;42(10):12312-22.
18. Kingsbury BFK, Li K. A morphological study of ceramic hollow fibre membranes. *J Membr Sci.* 2009;328(1-2):134-40.
19. Machado PST, Habert AC, Borges CP. Membrane formation mechanism based on precipitation kinetics and membrane morphology: flat and hollow fiber polysulfone membranes. *J Membr Sci.* 1999;155(2):171-83.
20. Gitis V, Rothenberg G. *Ceramic membranes.* Weinheim: Wiley-VCH; 2016.
21. Rahaman MN. Ceramic processing and sintering. In: Rahaman MN. *Powder consolidation and forming of ceramic.* 2nd ed. Boca Raton: CRC Press; 2003. p. 330-44.
22. Xu N, Liu Z, Zhang Y, Qiu H, Kong L, Tang X, et al. Fast synthesis of thin all-silica DDR zeolite membranes by co-template strategy. *Microporous Mesoporous Mater.* 2020;298:110091.
23. Nguyen NM, Le QT, Nguyen DPH, Nguyen TN, Le TT, Pham TCT. Facile synthesis of seed crystals and gelless growth of pure silica DDR zeolite membrane on low cost silica support for high performance in CO₂ separation. *J Membr Sci.* 2021;624:119110.

Supplementary Material

The following online material is available for this article:

Appendix A - CO₂ and CH₄ sorption test.